JOURNAL OF MAGNETIC RESONANCE 60, 337–341 (1984)

NMR Imaging in Solids by Multiple-Quantum Resonance

A. N. GARROWAY,* J. BAUM, M. G. MUNOWITZ, AND A. PINES

Department of Chemistry and Materials and Molecular Research Division, Lawrence Berkeley Laboratory, University of California, Berkeley, California 94720

Received June 15, 1984

NMR imaging is now a well-established technique for studying biological systems (*1*). In its most general form, an imaging method uses a magnetic field gradient to encode the positions of the nuclear spins with a spatially varying Larmor frequency. Once the variations in resonant frequency have been decoded appropriately, an image of the nuclear spin density or, more generally, of any mix of NMR parameters can be created.

In a linear magnetic field gradient, g, the spread of frequencies across a thickness Δz is $g\Delta z$. If features on the order of Δz are to be resolved, then the externally imposed field, $g\Delta z$, must itself be resolved relative to any background or internal field. For solids, the dominant background field is usually the local dipolar field, B_L. In biological systems familiar from ^{1}H imaging, rapid isotropic molecular motion often averages these internal dipolar fields to zero. However, in a strongly protonated solid, where molecular motion is restricted, a typical value for B_L might be 5 G so that a gradient greater than 50 G/cm (0.5 T/m) would be needed to achieve a resolution of 1 mm. One approach (*2–4*) to this problem is to reduce the effective local field by a multiple-pulse line-narrowing sequence (*5, 6*). The alternative approach is to leave the local field untouched, but to impose a gradient large enough to meet the condition $g \gg B_L/\Delta z$. In this communication, we demonstrate a prototype imaging experiment for solids based in spirit on this "brute force" method of increasing the gradient, but which relies instead on the properties of multiple-quantum NMR transitions (*7, 8*) to increase the effective gradient strength by an order of magnitude. Specifically, we intensify the effect of the gradient upon the evolution of the spin system by creating high-order multiple-quantum coherences and following their development in the static field gradient. A multiple-quantum coherence of order $n = M_i - M_j$, where M_i and M_j are the magnetic-quantum numbers for high-field states $|i\rangle$ and $|j\rangle$, evolves n times more rapidly in an inhomogeneous field than the usual single-quantum coherence. That is, if a single-quantum transition in the presence of a field gradient appears with resonance offset $\Delta\omega$, then an n-quantum transition appears at $n\Delta\omega$. The effective local dipolar fields are, however, roughly comparable for high- and low-order coherences in very large

* Permanent address: Code 6120, Chemistry Division, Naval Research Laboratory, Washington, D.C. 20375.

0022-2364/84 $3.00

spin systems. This apparent n-fold increase in gradient strength permits rather modest gradients to be used, provided high-order coherences are monitored. This feature has been exploited previously in NMR diffusion measurements (*9, 10*).

The multiple-quantum pulse sequence, shown in Fig. 1, is partitioned into preparation, evolution, mixing, and detection periods. The basic cycle of rf pulses is ($xxxx\bar{x}\bar{x}\bar{x}\bar{x}$), where x and $\bar{x}$ are $\pi/2$ pulses with phases of 0 and 180°, respectively. With the pulse spacing as shown in the figure, the zeroth-order average homonuclear dipolar Hamiltonian is

$$\mathcal{H}^{(0)} = \frac{1}{3}(\mathcal{H}_{yy} - \mathcal{H}_{xx}) = -\sum_{i<j} D_{ij}(I_{yi}I_{yj} - I_{xi}I_{xj}), \qquad [1]$$

under which coherences of even order can develop in a strongly coupled dipolar system (*11, 12*). The coherences then evolve freely for a time t_1 under the influence of the resonance offset and dipolar Hamiltonians,

$$\mathcal{H} = -\sum_i \Delta\omega_i I_{zi} - \sum_{i<j} D_{ij}(3I_{zi}I_{zj} - \mathbf{I}_i \cdot \mathbf{I}_j). \qquad [2]$$

A phase shift of 90° in the rf pulses creates a time-reversed mixing period (*11–13*), which is followed by detection of the magnetization using conventional methods. Our detection scheme employs spin-temperature inversion (*14*) to reduce artifacts from receiver ringing. One point is sampled for each value of evolution time, and the resulting signal is Fourier transformed against t_1. Separation of the multiple-quantum orders according to n is accomplished via the method of time-proportional phase incrementation (*15, 16*) of the pulses in the preparation period. Finally, we alternate the phases of the preparation pulses by 180° to remove any imperfections due to odd-order multiple-quantum contributions (*17*).

In imaging experiments the pulse sequence must work properly under the resonance offsets created by the dc field gradient; in this regard the present pulse sequence ($xxxx\bar{x}\bar{x}\bar{x}\bar{x}$) is superior to the cycle ($xx\bar{x}\bar{x}\bar{x}\bar{x}xx$) used earlier (*11, 12*).

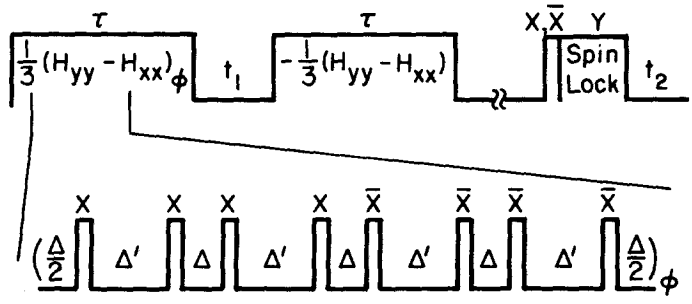

FIG. 1. The multiple-quantum pulse sequence. The preparation and mixing periods (τ), composed of cycles of eight $\pi/2$ pulses with duration t_p and rf phases x and $\bar{x}$, produce average Hamiltonians as shown for $\Delta' = 2\Delta + t_p$. To separate multiple-quantum orders, the relative phase ϕ between preparation and mixing is incremented in proportion to the evolution time t_1. About 1 ms after the end of the mixing the z component of magnetization is monitored with an x pulse and a 100 μs spin-locking pulse. The time-domain data are Fourier transformed against t_1 to produce the multiple-quantum spectra of Fig. 3.

Though the (zeroth order) average dipolar and resonance offset Hamiltonians are the same for both cycles, the symmetrization of the present sequence guarantees that the odd-order correction terms in the Magnus expansion vanish (*5, 6, 18*).

The phantom used in the multiple-quantum experiment is composed of three parallel glass melting point tubes (1.3 mm i.d., 1.65 mm o.d.), arranged linearly. The center tube is empty, while the outer tubes are loaded with a 4 mm length of compressed adamantane. The sample, consisting of the two cylindrical adamantane plugs (1.3 mm dia. × 4 mm) separated by 2.0 mm, is aligned with its cylindrical axes perpendicular to the z-axis field gradient, as is pictured in the inset of Fig. 2.

Figure 2 shows the 360 MHz ^{1}H single-quantum adamantane spectrum with and without a 48 mT/m field gradient. Although the gradient, which amounts to 20 kHz/cm, broadens the line from 12 kHz (full width at half height) to 14.5 kHz, the signals from the two adamantane plugs remain unresolved. The corresponding multiple-quantum spectra of the adamantane phantom are in Fig. 3. The main peaks represent multiple-quantum coherences out to $n = 14$. Very high-order coherences ($n > 60$) can be prepared and detected in adamantane but here we have selected, somewhat arbitrarily, a preparation time ($\tau = 396$ μs) which is sufficient to excite transitions up to n approximately 20 with reasonable intensity (*19*).

Figure 3 clearly demonstrates the attraction of imaging by multiple-quantum resonance. Peaks from the two adamantane plugs just begin to separate at $n = 4$, and are well resolved out at $n = 10$, where the gradient is effectively 10 times larger than for single-quantum coherence.

The multiple-quantum approach also possesses another interesting advantage, which derives from the separation of the evolution and detection periods: the spins

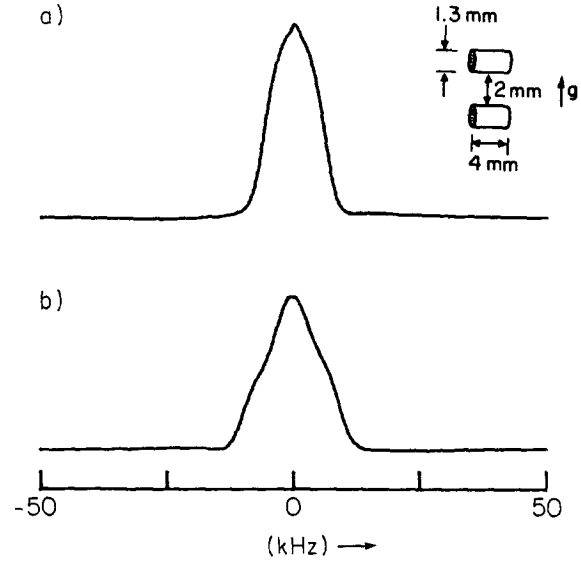

FIG. 2. Adamantane ^{1}H (single-quantum) spectra with (b) and without (a) a z gradient of 20 kHz/cm. Sample geometry is shown in the inset. The applied gradient is inadequate to resolve the signals from the two adamantane plugs.

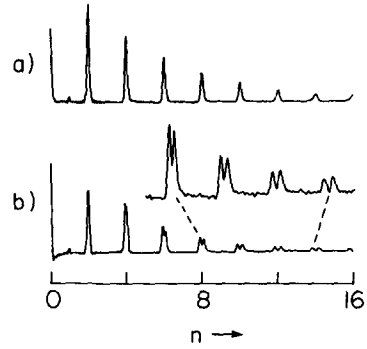

FIG. 3. Adamantane ^1H multiple-quantum spectra with (b) and without (a) a static z gradient. The preparation and mixing times (cf. Fig. 1) are 396 μs, corresponding to 6 cycles of the 8-pulse sequence with 3 μs $\pi/2$ pulses. The t_1 increment is 100 ns and the phase increment is $2\pi/32$; this separates each order by 312.5 kHz. For clarity the vertical scale has been expanded for orders 8–14. Even with a small gradient (20 kHz/cm) the two adamantane plugs can be resolved.

are labeled by the static gradient during the evolution period t_1, but are detected later during the t_2 interval. Consequently, while the bandwidth of the evolution frequencies during t_1 might be very great (say 10 MHz) to facilitate clean separation of the orders, no thermal noise is admitted during this interval. Any thermal noise comes to the receiver during the t_2 interval, but the bandwidth can actually be very narrow here. For imaging, this substantial benefit of the separation of evolution and detection is analogous to the advantage of a pulsed gradient over a steady gradient in diffusion measurements (*20*). Realization of this advantage requires that t_1 noise (*8*, p. 199 ff), due to fluctuations in the preparation and mixing periods, be minimized.

We have demonstrated here the essential feature of ^1H imaging by multiple-quantum NMR in strongly coupled solids: spatial resolution is enhanced considerably by the increased effective magnetic gradient seen by high-order coherences. Although we have displayed transitions of many orders, in an actual imaging scheme it might be advantageous to use only one order. Techniques of multiple-quantum filtering (*21*) and of selective preparation (*11*) suggest themselves.

ACKNOWLEDGMENTS

Thanks go to D. P. Weitekamp for helpful discussions concerning t_1 noise. One of us, A.N.G., was supported by the advanced research program of the Naval Research Laboratory. This work was supported by the U.S. Department of Energy through the Director's Program Development Funds of the Lawrence Berkeley Laboratory under Contract DE-AC03-76SF00098.

REFERENCES

1. (*a*) P. MANSFIELD AND P. C. MORRIS, "Advances in Magnetic Resonance," Suppl. 2, "NMR Imaging in Biomedicine," Academic Press, New York, 1982, and references therein; (*b*) L. KAUFMAN, L. E. CROOKS, AND A. R. MARGULIS, Ed., "Nuclear Magnetic Resonance in Medicine," Igaku-Shoin, New York, 1981; (*c*) P. A. BOTTOMLY, *Rev. Sci. Instr.* **53**, 1319 (1982); (*d*) E. R. ANDREW, *Accts. Chem. Res.* **16**, 114 (1983).
2. P. MANSFIELD, P. K. GRANNELL, A. N. GARROWAY, AND D. C. STALKER, "Proc. 1st Spec. Colloque Ampere" (J. W. Hennel, Ed.), p. 16, Krakow, 1973.

3. P. MANSFIELD AND P. K. GRANNELL, *J. Phys. C.* **6,** L 442 (1973).
4. R. A. WIND AND C. S. YANNONI, *J. Magn. Reson.* **36,** 269 (1979).
5. M. MEHRING, "Principles of High Resolution NMR in Solids," 2nd ed., Springer-Verlag, New York, 1983.
6. U. HAEBERLEN, "Advances in Magnetic Resonance," Suppl. 1, "High Resolution NMR in Solids: Selective Averaging," Academic Press, New York, 1976.
7. G. BODENHAUSEN, *Prog. Nucl. Magn. Reson. Spectrosc.* **14,** 137 (1981).
8. D. P. WEITEKAMP, *Adv. Magn. Reson.* **11,** 111 (1983).
9. J. F. MARTIN, L. S. SELWYN, R. R. VOLD, AND R. L. VOLD, *J. Chem. Phys.* **76,** 2632 (1982).
10. D. ZAX AND A. PINES, *J. Chem. Phys.* **78,** 6333 (1983).
11. W. S. WARREN, D. P. WEITEKAMP, AND A. PINES, *J. Chem. Phys.* **73,** 2084 (1980).
12. Y.-S. YEN AND A. PINES, *J. Chem. Phys.* **78,** 3579 (1983).
13. W.-K. RHIM, A. PINES, AND J. S. WAUGH, *Phys. Rev. B* **3,** 684 (1971).
14. E. O. STEJSKAL AND J. SCHAEFER, *J. Magn. Reson.* **18,** 560 (1975).
15. G. DROBNY, A. PINES, S. SINTON, D. P. WEITEKAMP, AND D. WEMMER, *Faraday Symp. Chem. Soc.* **13,** 49 (1979).
16. G. BODENHAUSEN, R. L. VOLD, AND R. R. VOLD, *J. Magn. Reson.* **37,** 93 (1980).
17. A. PINES, D. WEMMER, J. TANG, AND S. SINTON, *Bull. Am. Phys. Soc.* **23,** 21 (1978).
18. U. HAEBERLEN AND J. S. WAUGH, *Phys. Rev.* **175,** 453 (1968).
19. J. BAUM, M. G. MUNOWITZ, A. N. GARROWAY, AND A. PINES, *J. Chem. Phys.*, submitted for publication.
20. E. O. STEJSKAL AND J. E. TANNER, *J. Chem. Phys.* **42,** 288 (1965).
21. U. PIANTINI, O. W. SØRENSEN, AND R. R. ERNST, *J. Am. Chem. Soc.* **104,** 6800 (1982).